Report 9

Mathematically Modeled Comparison of Fischer-Tropsch Reactor System

G. J. Thompson
UOP Inc.

MATHEMATICALLY MODELED COMPARISON OF FISCHER-TROPSCH REACTOR SYSTEMS

by

Gregory J. Thompson, Anthony G. Vickers and Peter R. Pujado

UOP Process Division
UOP Inc.
Des Plaines, Illinois

INTRODUCTION

Experience in the last several decades has strengthened forecasts that a significant portion of our future transportation fuel requirements will be met by the conversion of coal. The Department of Energy has encouraged the development of processes which will produce usable fuels either by the direct or indirect liquefaction of coal. As part of this overall effort, DOE asked UOP to apply their expertise in process research and process design to evaluate four reactor systems available for the indirect liquefaction of coal via Fischer-Tropsch technology. Maximization of gasoline was the objective. The four systems were as follows:

Entrained Bed Reactor

Typical of this system is the Synthol reactor developed by Pullman Kellogg and used at Sasol. Sasol employs a promoted iron catalyst processing a hydrogen rich synthesis gas to produce liquid fuels.

Tube-Wall Reactor

This reactor system was developed by the Bureau of Mines (now known as Pittsburgh Energy Technology Center). Iron catalyst is coated on heat exchange tubes by flame or plasma spraying.

Slurry Reactor

This reactor was originally developed by Koelbel and others using a promoted iron catalyst.

Oil Circulation - Ebullating Bed Reactor

This reactor system has been utilized by Chem-Systems for methanation and synthesis of methanol.

These systems are shown schematically in Figure 1.

The results of this study are published under DOE Contract No. DEAC01-78ET10159 (1).

A reaction engineering approach was used to identify inherent strengths and weaknesses of the first three of the four reactor systems, thereby providing guidance regarding their potential. A process design approach was also used for considerations of size and cost differences, scale-up problems, general operability, etc. This paper is limited to the reaction engineering results with emphasis placed on the mechanism development and modeling. Models were developed for the entrained bed, tube-wall and slurry reactors.

MECHANISM

Anderson, et al. (2), Vannice (3), Catalytica Associates, Inc. (4), Oak Ridge (5), and Ponec (6), have all given excellent reviews of the existing theories on mechanisms for the Fischer-Tropsch reaction. In general, the vast majority of the data is discussed in terms of three mechanisms: the hydroxy-carbene mechanism, the formyl mechanism, and the carbide mechanism. At various points in Fischer-Tropsch history, each of these has been generally favored over the other two, and none of them can be clearly discounted from consideration. Even though each has its own distinctive active intermediate, there is still a great deal of commonality among the mechanisms.

This commonality is the foundation for the four minimum criteria which must be met to adequately describe the Fischer-Tropsch mechanism (1):

1. The mechanism must be a polymerization process.

2. The mechanism must be consistent with the generation of normal paraffins and olefins as primary products.

3. The mechanism must reflect the non-selective nature of the carbon number distribution as described by the Schulz-Flory distribution (9).

4. The mechanism should incorporate an equilibrium between the olefins on the catalyst sites and the olefins in the surrounding gas or liquid (20, 21).

Figure 2 is a schematic representation of the mechanism used in all the reactor models. M represents an "active" metal site. Whether M is a carbide, hydroxy-carbene, or a formyl structure is not important. It is merely a location where chain propagation can occur. The polymerization process proceeds by addition of CO and hydrogen to an alkyl chain, $M(CH_2)_{n-1}H$, forming another alkyl chain one carbon longer, $M(CH_2)_nH$, while liberating H_2O. This process is continued from $M(CH_2)_nH$ to $M(CH_2)_{n+1}H$, and so forth.

Two reactions are responsible for the production of the primary products. The first is the hydrogenation of an alkyl chain of any length to form a paraffin. The second is an equilibrium adsorption-desorption step to form an olefin. In both cases, when the active intermediate is "terminated", another initiation site, MH, is created, which can again participate in chain growth by reacting with CO and H_2. The mechanism, therefore, operates with a constant number of active catalyst sites. This is important if the mechanism is expected to reflect a Schulz-Flory distribution of products.

In the development of this mechanism and in the development of the rate expressions which describe the mechanism, some important assumptions were made. These were as follows:

1. Since oxygenated products, excluding H_2O and CO_2, seem to be formed in a manner similar to olefins and since the quantity formed is small for most Fischer-Tropsch catalysts, oxygenates are not considered at this time.

2. Branched olefins and paraffins are considered to be produced from the recoordination of olefins, i.e., the reattachment of olefins to the metal site. Recoordination is part of the proposed mechanism. However, distinction between recoordination of olefins in the branched form versus the unbranched form is not made.

3. Aromatics are considered to be small enough fractions of the total product to be eliminated from consideration at this time.

4. Catalyst deactivation is not considered.

5. The formation of free carbon is not considered, neither is the second route to methane through free carbon suggested by Dry (7).

6. The Schulz-Flory assumption that "All hydrocarbon species on the catalyst surface have an equal probability to add a carbon and form an oligomer one carbon longer," in kinetic terms suggests that the rate constant for polymerization is a constant function for all carbon numbers. This assumption is adopted not only for the polymerization rate constants but also for the paraffin termination and olefin formation rate constants.

7. The powers on all reactant and product concentration terms in the mechanism are assumed to be unity.

8. The pseudo-steady state assumption is used on the rates of formation of all metal site complexes.

9. The total number of "active" metal sites is assumed to be constant, i.e.,

$$[CAT] = MH + M(CH_2)H + \sum_{j=2}^{n} M(CH_2)_jH = \text{CONSTANT} \qquad (1)$$

Performance data in the literature show clear limitations to some of these assumptions. However, they are adequate for a first test of the mechanism on real data and for evaluation of gross product changes as a function of reactor design and operating conditions.

Based on these assumptions, then, the derivation of product rate expressions proceeds as follows. The rate of formation of the active species, $M(CH_2)H$, can be described by the following equation:

$$r_{M(CH_2)H} = k_p [MH] [CO] [H_2] - k_p [M(CH_2)H] [CO] [H_2] - k_H [M(CH_2)H] [H_2] \quad (2)$$

$M(CH_2)H$ can be defined in terms of MH with the assumption of pseudo-steady state:

$$[M(CH_2)H] = \frac{k_p [CO] [H_2]}{k_p [CO] [H_2] + k_H [H_2]} [MH] \quad (3)$$

In order to simplify the equations, let $D = k_p [CO] [H_2]$, $E = k_H [H_2]$ and $C = D/(D + E)$. This equation then simplifies to:

$$[M(CH_2)H] = C [MH] \quad (4)$$

In a similar manner, the rate of formation of $M(CH_2)_nH$ is described as:

$$r_{M(CH_2)_nH} = 0 = D [M(CH_2)_{n-1}H] - D [M(CH_2)_nH] - E [M(CH_2)_nH]$$
$$- k_o [M(CH_2)_nH] + \frac{k_n}{K_e} [C_nH_{2n}] [MH] \quad (5)$$

If one now collects terms and sets $A = D/(k_o + D + E)$ and $B = k_o/K_e\ (k_o + D + E)$, and solves for $[M(CH_2)_nH]$, the following equation results:

$$[M(CH_2)_nH] = A\ [M(CH_2)_{n-1}H] + B\ [C_nH_{2n}]\ [MH] \tag{6}$$

Using the method of successive substitution, Equations 4 and 6 lead to

$$[M(CH_2)_nH] = A^{n-1}\ C + B \sum_{i=2}^{n} A^{n-i}\ [C_iH_{2i}]\ \ [MH] \tag{7}$$

Substituting Equations 7 and 4 into Equation 1 and rearranging gives:

$$[MH] = \frac{[CAT]}{1 + C + \sum_{j=2}^{n} A^{j-1}\ C + B \sum_{i=2}^{j} A^{j-i}\ [C_iH_{2i}]} \tag{8}$$

Rate expressions for the products can be written as follows:

Methane

$$r_{CH_4} = k_H\ [M(CH_2)H]\ [H_2] \tag{9}$$

Paraffins $\quad n \geq 2$

$$r_{C_nH_{2n+2}} = k_H\ [M(CH_2)_nH]\ [H_2] \tag{10}$$

Olefins $n \geq 2$

$$r_{C_nH_{2n}} = k_o\,[M(CH_2)_nH] - \frac{k_o}{K_e}[C_nH_{2n}]\,[MH] \tag{11}$$

Substitution for $[M(CH_2)_nH]$ in these expressions leads to the final product rate expressions:

Methane

$$r_{CH_4} = C\,k_H\,[H_2]\,[MH] \tag{12}$$

Paraffins $n \geq 2$

$$r_{C_nH_{2n+2}} = \left(A^{n-1}\,C + B\sum_{i=2}^{n} A^{n-i}[C_iH_{2i}]\right)k_H[H_2]\,[MH] \tag{13}$$

Olefins $n \geq 2$

$$r_{C_nH_{2n}} = \left[k_o\left(A^{n-1}\,C + B\sum_{i=2}^{n} A^{n-i}\,[C_iH_{2i}]\right) - \frac{k_o}{K_e}[C_nH_{2n}]\right][MH] \tag{14}$$

The simplified rate expression adopted for the water-gas shift is as follows:

$$r_{WG} = k_{WG}\left([CO][H_2O] - \frac{1}{K_{eWG}}[CO_2][H_2]\right)[CAT] \tag{15}$$

It is assumed that this reaction proceeds in parallel with the Fischer-Tropsch reaction. Since Fischer-Tropsch catalysts have shift activity, the rate of reaction is assumed to be proportional to the catalyst concentration [CAT]. However, as it is not known whether the shift reaction requires the same active metal site as the Fischer-Tropsch reaction, it was decided that it should not compete for the same catalyst sites. Therefore, in this study the shift reaction is not assumed to be proportional to available Fischer-Tropsch initiation sites [MH], neither does it influence their concentration. The importance of the shift reaction to the understanding of the differences between reactor systems is discussed later in this paper.

REACTOR MODELS

The mechanism described has been incorporated into all three reactor models with the following additional assumptions:

Tube-Wall Reactor

1. Gas flows in ideal plug flow through the reactor.
2. There are no mass transfer limitations in the gas phase.
3. The gas phase and the catalyst are at the same temperature.

Entrained Bed Reactor

1. Catalyst and gas move in ideal plug flow.
2. There is perfect contacting between solids and gas.
3. There are no mass transfer limitations either in the gas phase or within the catalyst particles.

Slurry Reactor

1. Liquid is completely back-mixed.
2. The system is isothermal.
3. Gas moves in ideal plug flow.
4. All reactions take place in the liquid phase.
5. Solids are evenly dispersed in the liquid phase.
6. Mass transfer limitations only exist in the liquid phase from the gas-bubble interface to the bulk liquid.
7. Gas and liquid are at equilibrium at the gas-liquid interface.

DATA FITTING PROCEDURE

The reliability of the mechanism was tested by fitting rate constants to data from all three reactors.

The first step in the data fitting procedure was to identify the variables to be fit. The assumption in the mechanism that each of the rate constants is a constant function for all carbon numbers results in the product distribution being dependent on three rate constants and an equilibrium constant. These are the polymerization rate constant, k_p, the hydrogenation rate constant, k_H, the forward rate constant for the olefin formation, k_O, and its corresponding equilibrium constant, K_e. These are the independent variables in the kinetic mechanism.

The next step was to characterize the product distribution using four corresponding dependent variables. Three of the four became obvious choices. An overall carbon balance of

the system could be represented by CO conversion. The distribution of these carbons in the product could be approximated by the degree of polymerization as calculated from a plot of ln X_n vs. n. (The slope was determined from the gasoline fraction, i.e., between carbon numbers 5 and 11.) The hydrogen balance could be represented either by hydrogen conversion or, since only olefins and paraffins are produced as products, by olefin-to-paraffin ratio. Unless one is willing to consider variations in rate constant or olefin-to-paraffin ratio with carbon number, the three variables mentioned above describe the product in its entirety. From considerations of availability of consistent experimental data, and the desire to use the simplest possible approach in this first modeling attempt, the number of dependent variables has been limited to these three. Unfortunately, trying to fit four independent variables with three dependent variables leads to an infinite number of solutions.

A variable study was, therefore, undertaken to determine if the product distribution was sufficiently insensitive to one of the independent variables to be set equal to a constant. This would reduce the problem to an equal number of independent and dependent variables, thus leading to a unique solution. This study was done in an ideal plug flow reactor under isothermal conditions. A typical result for a given set of rate constants is represented in Figure 3. Two results of the constraints imposed on the mechanism are reflected in this plot. The first is in the methane production. Both the olefins and the paraffins, individually, are represented as straight lines and, therefore, follow a Schulz-Flory relationship. However, since there is no olefin of carbon number unity, methane can not follow a Schulz-Flory relationship relative to the total carbon number distribution, i.e., sum of the olefins and paraffins.

The second result is the olefin-to-paraffin ratio. Weitkamp, et al. (8), have shown that, for an iron catalyst operating in a fluidized bed, the olefin-to-paraffin ratio remains approximately constant beyond carbon number five. This implies that the olefin and paraffin lines in Figure 3 are parallel. Although this appears to be the case, in fact, the lines are gradually

converging and the olefin-to-paraffin ratio is continually decreasing with carbon number. Later runs with back-mixed reactors did show a constant olefin-to-paraffin ratio above a carbon number of 10 and only a small decrease above a carbon number of 5. At the present time we are not sure whether predictions of olefin-to-paraffin ratio with the proposed mechanism are meaningful, or whether some variation of rate constants with carbon number will be necessary.

Figure 4 represents the results when, for a given set of k_p, k_H, and k_O values, the value of K_e was changed from low to high. The curvature of the olefin line is caused by the light olefins approaching their respective equilibrium values. This variance from the idealized Schulz-Flory distribution was not the original objective of the mechanism. Although the intent is not to minimize the importance of this approach to equilibrium, as a first approach to the problem the value of K_e has been arbitrarily fixed at a low value for the remainder of our work, so as to more closely approximate the Schulz-Flory distribution of products. After a value for K_e is imposed, the overall problem of fitting is reduced to three dependent variables and three independent variables and can be readily solved.

In addition to limiting the number of independent variables, the variable study provided information regarding the relative sensitivity of CO conversion, degree of polymerization, and olefin-to-paraffin ratio to the three remaining independent variables, k_p, k_O, and k_H (Table 1). CO conversion is obviously most influenced by k_p and was, therefore, chosen as its fitting parameter. The degree of polymerization and olefin-to-paraffin ratio were affected equally by k_H and k_O. An arbitrary decision was taken to fit k_H to the degree of polymerization and k_O to the olefin-to-paraffin ratio. However, the same results were achieved when the fitting parameters for k_O and k_H were reversed.

The preceding discussion has revolved around three unknown rate constants. Actually each rate constant contains two unknown parameters, i.e., the Arrhenius frequency factor and the activation energy. The Arrhenius equation can be written as:

$$k_T = k_o{}^o e^{-\Delta E/RT_a} \qquad (16)$$

where: k_T = rate constant at temperature, T_a

$k_o{}^o$ = frequency factor

ΔE = activation energy

R = gas constant

T_a = absolute temperature

For a given catalyst, the frequency factor and the activation energy are fixed and the rate constant varies only as a function of temperature. The values of $k_o{}^o$ and ΔE were determined from the standard Arrhenius plot of ln k_o versus $1/T_a$.

The rate expression for the water-gas shift reaction was given by Equation 15. Since the equilibrium constant is well known, the only variable that needs to be fit is the forward rate constant, k_{WG}. The CO_2 concentration was chosen as the fitting parameter, since the production of CO_2 is unique to the shift reaction.

RESULTS AND DISCUSSION

As mentioned previously, the Arrhenius activation energies were determined by fitting the frequency factors to data at different temperatures. The fitting parameters were CO conversion, degree of polymerization and olefin-to-paraffin ratio.

The tube-wall reactor system was chosen for this work; first, because the simplicity of the plug flow system made results easy to interpret, and, second, because consistent results at different temperatures were not available for the other reactor systems. Table 2 represents temperature data collected by Haynes, et al., of PETC (16) for the tube-wall reactor operating with flame sprayed taconite catalyst at 650 psig. The degree of polymerization for each of these sets of data was determined in the following manner:

1. The product was divided into the following components:

   a) C_1-C_4 (gas)

   b) C_5-C_{11} (gasoline)

   c) C_{12}-C_{25} (diesel)

   d) C_{26}+ (heavy)

2. The Schulz-Flory plot of degree of polymerization versus weight fraction shown in Figure 5 was used to determine which degree of polymerization most nearly approximated the actual data.

The olefin-to-paraffin ratio required special consideration. As mentioned earlier, it remains to be determined whether the mechanism can predict olefin-to-paraffin ratio as a function of carbon number. In order to avoid this problem, an artificial ratio of unity was used in each of the data fitting runs. This in effect reduced the number of independent variables to two, CO conversion and degree of polymerization. However, despite the deficiencies of this first, deliberately simplified approach, useful insight into the strengths and weaknesses of the various reactor systems was gained. The final information used as input for the tube-wall fitting is given in Table 3.

The frequency factor results versus temperature as well as the corresponding activation energies are given in Table 4. The values are based on a referene temperature of 1100 °R. As can be seen, excellent agreement in frequency factors was achieved. The largest variance (15.3%) is for the water-gas shift reaction. The smallest variance (2.5%) is for the polymerization rate constant. The activation energies are typical of those for catalyzed reactions.

Because of the limited temperature data available, the above procedure for determining activation energies could not be used for each reactor system. Consequently, the activation energies given in Table 4 were used without modification for the gas phase reactor systems. In the case of the slurry reactor, Satterfield and Way (22) have shown that for a system where the carrier liquid is completely inert to reaction and/or adsorption on the catalyst site, the liquid phase reaction rate constant can be related to the gas phase reaction rate constant by the following equation:

$$k_L = K \frac{V_G}{V_L} k_G \qquad (17)$$

where: k_L = liquid phase reaction rate constant

k_G = gas phase reaction rate constant

V_L = molar volume of liquid at reactor conditions

V_G = molar volume of gas at reactor conditions

K = vapor-liquid equilibrium constant, $K = \frac{y}{x}$

x = mole fraction in liquid

y = mole fraction in gas

Equations of this form were incorporated into the slurry mathematical model allowing k_G and the activation energies given in Table 4 to be used for the slurry system. The relatively good agreement obtained in fitting data for other reactor systems confirms that this is a reasonable assumption.

While the fixed bed reactor system is not one of the reactors to be compared in this study, an abundance of data is available from the tubular reactor developed by the Pittsburgh Energy Technology Center (10, 11), in which lathe turnings were used as catalysts. Since the tubular reactor model can be used for the fixed bed system, a comparison of the catalyst used in these two systems was made. The frequency factor fit for the lathe turning reactor was made on the basis of Experiment 26C of the PETC work (11). (See Table 5). The comparison is presented in Table 6.

At first glance, the fit results look quite different from the tube-wall results. However, upon closer analysis, two very interesting explanations emerge. The first is related to catalyst activity. The computer model performs its calculations using weight as its basis for catalyst concentration. Actually, for this catalyst which has very little pore volume, the catalyst activity is more closely related to the external surface area than to the weight. The surface area per unit weight of the lathe turning catalyst was compared to that of the tube-wall catalyst, and the ratio was found to be very close to the ratio of the frequency factors for the polymerization and for the water-gas shift rate constants. In other words, the high apparent activity of the lathe turning catalyst could be easily explained by the higher surface area available. The polymerization rate constant was therefore used as a basis to correct the frequency factors derived for the lathe turning catalyst to the catalyst surface area available in the tube-wall reactor. The corrected numbers are also shown in Table 6.

In spite of this correction, the agreements for the hydrogenation and for the olefin formation rate constants are still poor. This led to the second explanation. The lathe turning

catalyst used for fitting purposes was potassium promoted while the tube-wall catalyst was not. There is much evidence in the literature (2, 12) that suggests that potassium promotion increases the degree of polymerization of the product. Based on a comparison of frequency factors, this phenomenon might be explained by a reduction in the hydrogenation/termination rate, thereby producing a heavier product via additional polymerization. Weitkamp, et al. (8), have provided support to this theory by showing a significant shift from a paraffinic to olefinic product with the addition of potassium.

Additional support for these explanations is provided when similar comparisons are made for the slurry and entrained bed systems. Koelbel's (13) yields and operating conditions, shown in Table 7, were used for fitting the slurry system. The Kellogg Feasibility Study (14) was used as a basis for yields and some of the operating conditions for the entrained bed system. In the latter case, however, Sasol literature, as well as engineering judgment, was required to supplement some deficiencies in the available data. The final information used for fitting is given in Table 8.

Frequency factor derivations are given at the top of Table 9. Here again the magnitudes of the frequency factors for the polymerization rate constant were found to be roughly in proportion to the surface area availability of the catalyst. For example, the difference between the frequency factors for the slurry and entrained bed reactors could be explained by the average particle size of the catalyst being 30 and 40 microns, respectively. In addition, the surface area per unit weight of catalyst is very high for both these systems, and is reflected in the high frequency factors relative to the tube-wall system.

The bottom of Table 9 shows the values of frequency factors after correction for surface area availability relative to the tube-wall catalyst. The similarity of values for the lathe turning catalyst and for the slurry catalyst is significant. Both catalysts are potassium promoted and

this is reflected in the values for k_H^o and k_o^o. While the entrained bed values are not as close, they are still in reasonable agreement, considering the lack of a consistent set of operating data for fitting. The only frequency factor which is completely out of line is for the water-gas shift in the entrained bed system. A closer scrutiny of the data revealed a high concentration of CO_2 in the combined feed. As a result, water-gas shift was found to be at equilibrium throughout the entire reactor. It is obviously impossible to determine a forward rate of reaction when that reaction is at equilibrium. This value must, therefore, be disregarded.

The frequency factors used in the entrained bed and slurry variable studies are those listed at the top of Table 9. These produced the most favorable yield structures for their respective reactor systems. The tube-wall frequency factors, however, produced yield structures which were much too high in methane yield and much too low in gasoline yield. Conversely, the lathe turning values, although better, produced a yield structure which was too heavy. A compromise led to the final selection of the lathe turning values modified for slightly less potassium promotion. This was accomplished by increasing the hydrogenation frequency factor from 0.07 to 0.1. The values used were: $k_p^o = 73.0$; $k_H^o = 0.1$; $k_o^o = 0.00129$; and $k_{WG}^o = 205.0$.

A very important overall conclusion was drawn from reflecting on the data fitting results. That is, a single mathematical mechanism has been developed which, when incorporated into models of three completely different reactor systems, operating at completely different operating conditions, gave reasonable agreement on the rate constants associated with Fischer-Tropsch catalysts manufactured by several independent investigators. Also, the data with and without potassium promotion of the catalyst show that the mechanism will allow interpretation of yield differences resulting from different catalyst formulations. The reactor comparisons, therefore, proceeded with some confidence that the models can also be used to predict with reasonable accuracy the gross product distributions for each system.

Individual Reactor Studies

Extensive variable studies have been performed for each reactor system, and the results in their entirety were documented in DOE Contract No. DEAC01-78ET10159. In this paper, one result for each reactor has been selected for presentation.

Tube-Wall Reactor — Under DOE Contract No. E(49-18)-1775, Ralph M. Parsons Company (15) prepared a report which describes "The results of a conceptual design and economic evaluation for a conceptual Fischer-Tropsch plant responsive to U.S. demands and economic requirements." The Fischer-Tropsch synthesis reactor chosen for this study was the tube-wall system. The yield structure was based on Experiment 26C (Table 5) with the lathe turning catalyst mentioned earlier. The activity of the catalyst was determined from Experiment HCR-34 (Table 10) which studied flame sprayed magnetite. The final design selected by Parsons is given in Table 11. A comparison of this conceptual design with the PETC experimental data is given in Table 12. A critical analysis suggests that the activity selected for the conceptual design was very optimistic. The fit results presented in Table 6 earlier suggested that the polymerization activity, k_p^o, of lathe catalyst is very nearly the same as that for flame sprayed taconite catalyst. Haynes, et al. (16), have shown that taconite catalyst is significantly less active than magnetite catalyst and yields a higher molecular weight product. Closer examination of Experiments 26C and HCR-34 shows that potassium promoted magnetite has a much lighter yield structure than potassium promoted lathe turnings. Potassium promoted taconite must, therefore, be used as catalyst if the lathe turning yield structure represented in the Parsons study is desired.

A study was undertaken to compare the Parsons reactor design and operating conditions, which were based on flame sprayed magnetite, to that which would result from a flame sprayed, potassium promoted taconite (or lathe turning equivalent). The results are given in

Table 13. Case 1 used the Parsons reactor design. (The GHSV is not quite the same, but this is the result of using bare tubes in the model while Parsons used finned tubes.) The lower activity and heavy product distribution of the taconite catalyst is reflected in a low CO conversion and a high degree of polymerization. In Case 2, the temperature increased to 640 °F and the size of the reactor is increased until a CO conversion on fresh feed of 90% is achieved. The predicted yields are then close to what was used in the Parsons sutdy, but the total syngas conversion ($CO + H_2$) remains lower than that used by Parsons, and the reactor is roughly twice the size with an operating temperature considerably higher.

This study is presented as an example of how the reactor models can be used to interpret experimental data, and predict what may be the results of using commercial scale equipment. The design shown in Table 13 is not represented as a optimized design for a tube-wall reactor. In fact, it is doubtful that this reactor could operate at 640 °F and the H_2/CO ratio indicated without significant problems of free carbon formation.

Entrained Bed Reactor -- Because of the complexity of the entrained bed system, the effect of a single variable change is difficult to study. For example, the definition of reactor temperature is a problem due to the nature of the heat removal system. Given a fixed inlet temperature, the outlet temperature, and consequently the average reactor temperature, could be changed by adjusting the cooling oil rate to the heat removal coils. An illustration of the models prediction of this effect on CO conversion and degree of polymerization can be seen in Figures 6 and 7. As cooling oil rate is reduced, reactor ΔT increases, resulting in an increased conversion and decreased degree of polymerization.

The limited flexibility inherent to the entrained bed reactor system created another example of the difficulty in changing a single variable. An attempt was made to reduce the recycle ratio to below one. When this was done, the partial pressures of both hydrogen and carbon monoxide in the combined feed increased. In addition, the superficial velocity in the reactor

was reduced resulting in increased residence time and higher catalyst concentrations. The net result is a temperature runaway before the first set of exchangers is reached.

These types of complexities led to two guidelines for conducting variable studies on the Kellogg design:

1. A constant ΔT across the reactor was maintained by adjusting cooling oil rate equally between the two heat removal sections, and

2. The rate and composition of hydrocarbons in the recycle gas were held constant and equal to that shown for Kellogg.

The influence of catalyst circulation rate is unique to the entrained bed system. Yerushami, et al. (17), have shown that for a fixed gas rate, if the catalyst circulation rate is increased, i.e., the catalyst loading is increased (lbs catalyst per ft^3 of gas), additional slippage will occur resulting in higher catalyst density in the reactor. This effect can be seen in Figure 8 for the base case conditions. The increased catalyst density leads to higher conversions (Figure 9), but apparently has little effect on the degree of polymerization.

The influence of solids loading on catalyst density led to a term, β, defined as standard cubic feet of fresh feed per hour per pound of catalyst within the reactor being chosen as a correlating factor rather than gas hourly space velocity (GHSV). Although GHSV may be a measure of space utilization efficiency, it is not an accurate measure of catalyst utilization efficiency for the entrained bed reactor. CO conversion decreases dramatically with increasing β (Figure 10), while degree of polymerization increases only slightly.

Slurry Reactor — The question of whether there are mass transfer limitations in the slurry reactor has received significant attention in the literature but, to date, has not been answered conclusively. A set of conditions suggested by Koelbel (13) was used to determine the sensitivity of two mass transfer parameters on CO conversion and degree of polymerization. The first parameter, the specific interfacial area, is a measure of the bubble surface area available per volume of reactor space. The second parameter, the mass transfer rate constant, fixes the rate of mass transfer for a given component.

Although some work has been done on determining specific interfacial areas in slurry systems, values reported are at best approximations. The value chosen for the majority of these studies, 300 ft^2/ft^3, is consistent with those reported by Koelbel (18) and Deckwer (19). A study was made to determine what would be the influence of a 20% lower interfacial area. Figures 11 and 12 represent results with an interfacial surface area of 240 ft^2/ft^3. The CO conversion is reduced roughly 0.2-0.8%, but the degree of polymerization is not affected at all. The latter result is not surprising since the interfacial area should influence the rate of mass transfer of all components equally.

In order to study the influence of mass transfer rate on CO conversion and degree of polymerization, the values of the mass transfer rate constant, k_L, for hydrogen and CO were individually adjusted 20% above and below their respective base values. The results are presented in Figure 13. As can be seen, neither the mass transfer rate constant for H_2, nor the constant for CO has a dramatic effect on either CO conversion or degree of polymerization.

These results do not support the conclusion that the slurry reactor operating at Koelbel's conditions is mass transfer limited.

Reactor Comparison

As in the case of the variable studies, an extensive number of reactor comparisons have been made. Here again, only two of particular interest are chosen for presentation.

One of the most important questions asked during the evaluation of these reactor systems was — How efficiently does each reactor system convert CO and H_2 to usable product? To answer this question, a comparison was made at "base case" conditions for each reactor system. In the case of the entrained bed and slurry reactors, the base case was the Kellogg (14) and Koelbel (13) designs, respectively. In the case of the tube-wall reactor, the base case consisted of feed and product yields from the Parsons design modified to represent potassium promoted taconite as catalyst.

Table 14 represents reactant conversion and product yields per mole of fresh feed and per mole of CO plus H_2 converted. A comparison of total weight of hydrocarbon produced per mole of fresh feed suggests that the entrained bed reactor makes more product than the slurry reactor, which makes more product than the tube-wall reactor. Although these numbers may represent the performance of each specific reactor, they do not reflect the performance of the overall reactor systems for conversion of synthesis gas. For example, the entrained bed and tube-wall systems both have high H_2/CO ratio feeds relative to the slurry system. These ratios must be obtained by conducting the water-gas shift reaction prior to the Fischer-Tropsch reaction. This consumption of CO to CO_2 is not reflected when put on a fresh feed basis.

If moles of CO plus H_2 converted is used as a basis, the influence of feed compositions and water-gas shift can be eliminated. For every mole of CO converted via water-gas shift, for example, a mole of H_2 is produced and, therefore, the sum of H_2 plus CO remains unchanged.

A comparison of total weight of hydrocarbon produced on this basis shows only minor differences between reactor systems. However, the efficiency with which the shift reaction is being used is clearly shown by the relative consumptions of H_2, CO, H_2O, and CO_2.

In the case of the entrained bed system, the CO_2 level in the combined feed, caused by high concentrations in the recycle gas, is so high that the shift reaction is at equilibrium, i.e., no CO_2 produced. Virtually every mole of CO entering the reactor is converted to hydrocarbon product. On the other hand, not one mole of H_2 is being produced within the reactor. The net result is that a large water-gas shift system is required upstream of the entrained bed reactor in order to supply the necessary hydrogen for feed.

In contrast, the shift reaction in the slurry reactor is far from equilibrium as reflected by the CO_2 produced. A significant portion of the CO is being converted to CO_2 in order to produce the necessary hydrogen, but the weight of hydrocarbon produced is equivalent or perhaps slightly greater than the other systems. Also the shift reaction is taking place in the same vessel as the Fischer-Tropsch reaction. Auxiliary equipment for adjustment of H_2/CO ratio is, therefore, not necessary, and as steam for the shift system does not have to be produced, an overall advantage in thermal efficiency will result.

The tube-wall reactor falls in between. This reactor requires a high H_2/CO ratio in the feed and, therefore, requires auxiliary shift reaction equipment. At the same time, the CO_2 content of the feed is not high enough to prevent the production of unneeded H_2 at the expense of CO. The combination of these two effects causes the tube-wall system to produce significantly less hydrocarbon per mole of fresh feed than the other systems.

There are few operating variables that have a more dramatic effect on degree of polymerization than temperature (Figure 14). The reason lies in understanding the competition

between rates of polymerization and hydrogenation as it relates to the rate constants. The rates of polymerization and hydrogenation are proportional to Arrhenius rate constants with activation energies of 26,430 and 28,825 Btu/lb mole, respectively. An increase in temperature from 500 °F to 600 °F increases the polymerization and hydrogenation rate constants by factors of 3.71 and 4.17, respectively. Thus, the ratio of rate of polymerization to rate of termination decreases to 0.89 of its original value, which causes the degree of polymerization to decrease with increasing temperature.

Although the above discussion satisfactorily explains the direction of change, it does not explain the insensitivity of the entrained bed reactor system relative to the slurry or tube-wall systems. The slurry reactor was defined as being isothermal. Although the tube-wall reactor was not defined in this manner, the heat transfer coefficient for heat removal was such that nearly isothermal conditions were attained. The entrained bed system was the only system that had three distinct areas of increasing temperature through the reactor. The influence of increasing temperature on degree of polymerization was found to be greater at low temperatures than at high temperatures. Since the ΔT across the entrained bed reactor was held constant at 36 °F, the decrease in degree of polymerization caused by this ΔT at an inlet temperature of 500 °F was greater than at 600 °F. The result is a reduced sensitivity.

Response of Degree of Polymerization to Space Velocity

One puzzling result of the modeling work was the prediction that the degree of polymerization of the product would decrease as the residence time increased. This was true regardless of reactor type and occurred within the entire range of Fischer-Tropsch operating conditions. A polymerization product intuitively becomes heavier the lower the reactor gas hourly space velocity.

The key to understanding this result lies in the competition between polymerization and termination. The longer the growing chain remains at a catalyst site before being hydrogenated to a paraffin, or leaves the catalyst site as an olefin, the higher the degree of polymerization and the molecular weight of the product. This, therefore, will be a function of the relative rates of these processes.

The polymerization term ($D = k_p [CO] [H_2]$) is a function of the partial pressure of both CO and H_2. The irreversible hydrogenation to paraffins term ($E = k_H [H_2]$) is only a function of hydrogen partial pressure. Because of the water-gas shift reaction, the CO conversion through a reactor is much higher than the hydrogen conversion, resulting in the partial pressure of CO dropping much more across the reactor than that of hydrogen. For example, the volumetric percentage of CO may go from 35% at the inlet to 5% at the outlet, while the hydrogen goes from 65% to 45%. This will result in the polymerization term falling to 10% of that at the inlet while the hydrogenation term is still 70% of that at the inlet. The ratio has, therefore, changed by a factor of 7, and this will have the effect of causing a falling molecular weight of product, and a lower degree of polymerization with increasing conversion.

The other factor that can influence the molecular weight of the product is related to the reversible termination reaction to form olefins. The effect of this reaction is to influence the proportion of CO reacting to initiate new chains compared to that elongating existing chains. As the concentration of olefins in the vapor phase increases, the reverse reaction will slow down the rate of release of olefins to the vapor phase. However, in the investigations carried out to date with the reactor models, two factors combine to make this effect insignificant. First, the concentration of olefins is still quite low at the outlet of the reactor in all cases, because of the high concentrations of H_2, CO_2 and H_2O, which are inherent to the reaction system. (The slurry system has the highest olefin concentration at the outlet, but it is still less than 5 mol-%.) The rate of the reverse reaction, therefore, will be low because of the low

olefin concentrations. Second, the value of K_e used in these studies was not determined from experimental data. (The selected value is discussed earlier in this paper.) If experimental data support a lower value of K_e (i.e., a higher rate constant for the reverse reaction), this can increase the influence of this effect. An investigation of the effect of olefin concentration on the degree of polymerization of the product will have to wait for further experimental data.

Table 15 provides an overall view of what happens with increasing CO conversion. Here the conversion at the reactor outlet was taken to 98.3%. The hydrogen content remains high while the olefins only reach 3 mol-%. The CO concentration decreases from 32 to 1 mol-%.

CONCLUSIONS

1. A mathematical mechanism has been developed which, when incorporated into models of three completely different reactor systems operating at completely different operating conditions with Fischer-Tropsch catalysts of different manufacture, gives reasonably good agreement on important rate constants derived from the experimental data published for these systems.

2. The mechanism, as demonstrated for potassium promoted catalyst, allows interpretation of yield differences resulting from different catalyst formulations..

3. As demonstrated in the Parsons study, the reactor models can be used to evaluate existing conceptual designs not only in terms of gross product yield but also in terms of reactor design and operating conditions.

4. The entrained bed reactor lacks the operating flexibility of the tube-wall and slurry reactor systems.

5. In the entrained bed reactor, catalyst circulation rate can be used as an operating parameter to adjust catalyst density within the reactor. Increased catalyst density increases CO conversion without significantly influencing the gross product yields.

6. The influence of mass transfer on the CO conversion and degree of polymerization in the Koelbel slurry reactor is small.

7. At the operating conditions proposed in the literature for these systems, the slurry reactor will inherently have a higher thermal efficiency than the entrained bed or tube-wall reactors, because of the more efficient use of the water-gas shift reaction.

8. Of all operating parameters (excluding catalyst), temperature has the strongest influence on gross product yields.

9. The sensitivity of product yields to temperature is best utilized in the slurry reactor. Its three-phase nature allows the production of liquid product at low temperatures.

10. Next to temperature, the largest influence on product yield is the relative concentration of H_2 and CO. This is caused by the competition between the rate of polymerization and the rates of termination, which are strongly dependent on the ratio of H_2 to CO.

11. Because of the success of this simplified mechanism in describing inherent strengths and weaknesses in a variety of Fischer-Tropsch reactor systems, work proceeds on eliminating some of the mechanism deficiencies, thereby providing additional support to conclusions already drawn and providing additional insight into product yields.

ACKNOWLEDGMENT

The authors would like to acknowledge R. E. Hildebrand of the Department of Energy for his advise and encouragement throughout this project. Additional thanks are given to Dr. D. S. Hacker of the University of Illinois (Chicago Circle) for his continued assistance and consultation.

NOMENCLATURE

[CAT]	catalyst concentration (lb/ft^3 reactor)
[MH]; [$M(CH_2)_2H$]	catalyst site concentration (lb/ft^3 reactor)
[CO]; [H_2]; [CO_2]; [H_2O]; [C_nH_{2n}]	component concentrations (moles/ft^3)
r	rate expression (moles/hr-ft^3 reactor)
k_p	polymerization rate constant [$(ft^3)_{Rx}$/lb-hr-moles]
k_H	hydrogenation rate constant (ft^3_{Rx}/lb-hr)
k_o	olefin equilibrium forward rate constant (moles/lb-hr)
k_{WG}	water-gas shift forward rate constant (ft^3_{Rx}/hr-mole)
K_e	olefin equilibrium constant (moles/ft^3 Rx)
K_{eWG}	water-gas shift equilibrium constant (unitless)
k^o	Arrhenius frequency factor
X_n	mole fraction of component n
β	standard cubic feet per hour per pound of catalyst

BIBLIOGRAPHY

(1) UOP Inc., "Comparison of Fischer-Tropsch Reactor Systems — Phase I," Final Report, DOE Contract No. DEA CO1-78ET10159.

(2) Anderson, R. B., Schultz, J. F., Hofer, L. J. E., and Storch, H.H., "Physical Chemistry of the Fischer-Tropsch Synthesis," Bulletin 580, U.S. Bureau of Mines, 1959.

(3) Vannice, M. A., "The Catalytic Synthesis of Hydrocarbons from Carbon Monoxide and Hydrogen", Sci. Eng., 14 (2), 153-191, (1976).

(4) Catalytica Associates, Inc., "Catalysis of CO-H_2 Reactions — A Criticai Analysis," Multiclient Study No. 1043, January, 1978.

(5) Oak Ridge National Laboratory Report, "Fischer-Tropsch Synthesis," March, 1979.

(6) Ponec, V., "Some Aspects of the Mechanism of Methanation and Fischer-Tropsch Synthesis," Catal. Rev. - Sci. Eng., 18 (1), 151-171, (1978).

(7) Dry, M. E., "Predict Carbonation Rate of Iron Catalyst," Hydrocarbon Processing, 59, 2, 92-94 (1980).

(8) Weitkamp, A. W., Seelig, H.S., Bowman, N.J., and Cady, W. L., "Products of the Hydrogenation of Carbon Monoxide over an Iron Catalyst," Industrial and Engineering Chemistry, 45, 2, (1953).

(9) Flory, P. J., "Principles of Polymer Chemistry", Cornell University Press, Ithaca, N.Y., 1967.

(10) Field, J.H., Bienstock, D., Forney, A.J., and Demski, R.J., "Further Studies of the Fischer-Tropsch Synthesis Using Gas Recycle Cooling (Hot-Gas-Recycle Process)," U.S. Dept. of the Interior, Bureau of Mines, 1961.

(11) Forney, A.J., Bienstock, D., Demski, R.J., "Use of a Large Diameter Reactor in Synthesizing Pipeline Gas and Gasoline by the Hot-Gas-Recycle Process," U.S. Dept. of the Interior, Bureau of Mines, 1962.

(12) Storch, H. H., Golumbic, N., and Anderson, R. B., "The Fischer-Tropsch and Related Syntheses," John Wiley and Sons, Inc., New York, N.Y., 1951.

(13) Koelbel, H., Ackerman, P., and Englehardt, F., "New Developments in Hydrocarbon Synthesis," Proceedings Fourth World Petroleum Congress -- Section IV/C, 1955.

(14) Pullman Kellogg, "Synthol Feasibility Study for Standard Oil Company (Indiana) — Base Case," J-5109, Revised Version, October, 1977.

(15) The Ralph M. Parsons Co., "Fischer-Tropsch Complex Conceptual Design/Economic Analysis," R & D Report No. 114, Interior Report No. 3, January, 1977, ERDA Contract No. E(48-18) - 1975.

BIBLIOGRAPHY (Continued)

(16) Haynes, W. P., Baird, M. J., Schehl, R. R., and Zawchak, M. F., "Fischer-Tropsch Studies in a Bench-Scale Tube-Wall Reactor Using Magnetite Raney Iron, and Taconite Catalyst," ACS Meeting, Anaheim, March 12-17, 1978.

(17) Yerushami, J., and Chankurt, J. T., "Further Studies of the Regimes of Fluidization," Powder Technology, 13, 187-205 (1979).

(18) Koelbel, H., and Palek, M., "The Fischer-Tropsch Synthesis in the Liquid Phase," Catalyst Reviews -- Science and Engineering, 21 (2), 225-274 (1980).

(19) Deckwer, W. D., Louisi, H., Zaidi, A. K., and Ralek, M., "Gas Holdup and Physical Transport Properties for the Fischer-Tropsch Synthesis in Slurry Reactor," AIChE, 72nd Annual Meeting, San Francisco, November 25-29, 1979.

(20) Caesar, P.D., Brennan, J.A., Gardwood, W.E., and Ciric, J., "Advances in Fischer-Tropsch Chemistry," Journal of Catalysis, 56, 274 (1979).

(21) Pichler, H., and Schulz, H., "Neure Erkemtnisse auf dem Gebiet der Synthese von Kohlenwasserstoffen aus CO and H_2," Chemie Ing. Techn., No. 18, 1162-1174 (1970).

(22) Satterfield, C. N., and Way, P. F., "The Role of the Liquid Phase in the Performance of a Trickle Bed Reactor," AIChE Journal, 18, 2, March, 1972.

TABLE 1

VARIABLE DEPENDENCE

Independent	Dependent: CO Conversion	Degree of Polymerization	Olefin-to-Paraffin Ratio
K_p	↑	↑	–
K_H	↑	↓	↓
K_o	↑	↓	↑

TABLE 2

EFFECT OF TEMPERATURE,
P = 650 psig, H_2/CO = 2.11

PETC Tube-Wall Data

T, °C (°F)	275 (526)	310 (589)	335 (634)
% CO Conversion	30.7	54.8	77.2
Product Distribution, Wt-%:			
$C_1 + C_2$	60.0	67.0	69.7
C_3	9.9	10.3	10.5
Gasoline ($C_3^=$ - < 204 °C)	24.1	20.6	14.2
Diesel (204 - 316 °C)	4.3	1.1	3.4
Fuel Oil (316 - 450 °C)	1.7	1.0	2.2
Wax (> 450 °C)	0	0	0
Gross Molar Flow Rate, (moles/hr x 10^4)	1.51	3.53	6.62

Values Used for Data Fitting

Degree of Polymerization	2.7	2.2	2.1
Olefin to Paraffin Ratio	1.0	1.0	1.0

TABLE 3

TUBE-WALL REACTOR FITTING

Fresh Feed Rate, moles/hr	0.009608
Composition, %	
H_2O	0.5
H_2	66.2
CO	31.0
CO_2	0.5
CH_4	1.9
J Factor (SCFH FF/ft^2 Cat Surface Area)	23.87
Reactor Dimensions	
Inside Diameter of Tube, ft	0.0402
Outside Diameter of Tube, ft	0.0875
Shell Diameter, ft	0.175
Length, ft	0.5
Catalyst Thickness, ft	0.00208

TABLE 4

TUBE-WALL FREQUENCY FACTORS

Temp, °C (°F)	275 (526)	310 (589)	335 (634)	Derived Activation Energies (Btu/lb mole)
Frequency Factors				
k_p^o [$(ft^3_{Rx})^2$/lb Cat-hr-mole]	73.3	71.5	73.0	26,400
k_{II}^o (ft^3_{Rx}/lb Cat-hr)	0.436	0.494	0.465	28,800
k_o^o (ft^3_{Rx}/lb Cat-hr)	0.0180	0.0203	0.0193	27,000
k_{WG}^o [$(ft^3_{Rx})^2$/lb Cat-hr-mole]	169.58	144.38	170.5	33,000

I = Input C = Calculated

	I	C	I	C	I	C
CO Conversion	30.7	30.7	54.8	54.9	77.2	77.2
Degree of Poly.	2.70	2.71	2.20	2.19	2.10	2.10
Olefin/Paraffin	1.00	1.00	1.00	0.988	1.00	0.981
CO + H_2 Conversion	28.4	27.3	51.1	46.0	66.1	59.2
CO_2 Molar Flow	1.51×10^{-4}	1.50×10^{-4}	3.53×10^{-4}	3.53×10^{-4}	6.62×10^{-4}	6.61×10^{-4}

Note: All frequency factors are based on a reference temperature of 1100 °R.

TABLE 5

EXAMPLE EXPERIMENTAL RESULTS
STEEL LATHE TURNINGS CATALYST (SLTC) FISCHER-TROPSCH RUNS

Item	Experiment 26 Period C
Catalyst Type	SLTC
Synthesis, hours	416 - 488
Reactor Conditions	
Fresh Feed Rate, scfh	1,214
Space Velocity, vol/vol/hr	607
Reactor Pressure, psig	405
Recycle to Fresh Feed:	
Total	27
Hot	25.5
Cold	1.5
CO_2 scrubbed	1.5
Reactor temperature, °F	
In Gas	552
Out Gas	610
Increment	58
Average Catalyst Temperature, °F	586
Maximum Catalyst Temperature, °F	622
H_2:CO Ratio, Fresh Gas	1.45
Results	
CO_2 Free Contraction, %	74.6
H_2 Conversion, %	73.7
CO Conversion, %	88.7
H_2 + CO Conversion, %	79.8
H_2: CO Ratio:	
Recycle Gas	3.35
Usage	1.21
Water Vapor in Recycle Gas, vol-%	7.0
Tail Gas Composition, vol-%(a)	
H_2	55.2
CO	16.5
N_2	1.2
CO_2	9.6

TABLE 5 (Continued)

Item	Experiment 26 Period C
Tail Gas Composition, vol-%[a]	
C_1	9.8
$C_2^=$	0.7
C_2	2.3
$C_3^=$	0.3
C_3	1.0
$C_4^=$	0.6
C_4	1.8
$C_5^=$	0.2
C_5	0.8
$C_6^=$	0
C_6	0
Yield, g/m^3 (H_2 + CO) Converted	
C_1	24
$C_2^=$	3
C_2	12
$C_3^=$	2
C_3	7
$C_4^=$	6
C_4	18
$C_5^=$	2
C_5	9
$C_6^=$	0
C_6	0
Oil	0.97
Aqueous	130
C_1 - C_3OH[b]	8
Other Oxygenates[b]	3
Water	119
CO_2	307
Hydrocarbon Recovery, g/m^3	191
Theoretical Recovery, g/m^3	201
Hydrocarbon Recovery, wt-%	
C_1 + C_2	19.4
C_3	3.5
Gasoline (C_3 = < 400°F)	59.0
Diesel Oil (400 to 600 °F)	9.1
Fuel Oil (600 to 842 °F)	6.2
Wax (< 842 °F)	2.8

(a) Dry basis.
(b) Calculated as hydrocarbons.

TABLE 6

TUBE-WALL vs. LATHE TURNINGS
FREQUENCY FACTORS

	Tube-Wall	Lathe Turning	Corrected Lathe Turning
k_p^o [$(ft^3_{Rx})^2$/lb Cat-hr-mole]	73.0	113.0	73.0
k_H^o (ft^3_{Rx}/lb Cat-hr)	0.465	0.108	0.070
k_o^o (ft^3_{kx}/lb Cat-hr)	0.0193	0.002	0.00129
k_{WC}^o [$(ft^3_{Rx})^2$/lb Cat-hr-mole]	170.0	318.0	205.0

Note: All frequency factors are based on a reference temperature of 1100 °R.

TABLE 7

OPERATING DATA AND RESULTS OF LIQUID-PHASE SYNTHESIS FOR ONE-STEP OPERATION WITH A SINGLE PASSAGE OF THE GAS OVER IRON CATALYSTS

Effective Reaction Space, volume suspension including dispersed gas, (λ)	10,000
Catalyst, kg Fe	800
Synthesis Gas Pressure, bar	12
Synthesis Gas, (volume ratio, $CO:H_2$)	1.5
Quantity of Synthesis Gas, Nm^3/h	2700
Linear Velocity of the Compressed Gases at Operating Temperature Referred to the Free Reactor Cross Section, cm/s	9.5
Total $CO + H_2$ used, Nm^3/h	2300
per m^3 of Reaction Chamber	230
per kg of Fe	2.6
Average Synthesis Temperature, °C	268
CO Conversion, %	91
$CO + H_2$ Conversion, %	89
Synthesis Products Referred to $CO + H_2$ used, g/Nm^3	
Hydrocarbons	
C_1^+	178
$C_1 + C_3$	12
C^{3+}	166
O-containing Products in the Synthesis Water, g/Nm^3	3
Space-time Yield of C_3^+ Products incl. O-products in 24 hours (kg/m^3 of reaction chamber)	930

TABLE 7 (Continued)

Composition of a Product from the Demonstration Plant
(Mode of Operation Adjusted for Gasoline Production)

	g/Nm^3 $CO + H_2$	Wt-% of Total Product C_1^+	% Olefin
Methane + Ethane	5.7	3.2	0
Ethylene	613	3.6	100
C_3	40.3	22.6	75-85
C_4	9.1	5.1	70-80
40-180°C Fraction	95.5	53.6	70
180-220 °C	7.1	4.0	45
220-320 °C	10.7	6.0	37
> 320 °C	3.3	1.9	7
Total	178.0	100.0	

TABLE 8

SLURRY AND ENTRAINED BED INPUT
FOR FITTING PURPOSES

	Slurry	Entrained Bed
Fresh Feed Rate, moles/hr	251.6	86,585.9
Composition, %		
H_2O	3.0	0.01
H_2	38.0	66.51
CO	54.0	27.71
CO_2	5.0	5.77
Recycle Rate, moles/hr	-	192,500.00
Composition		
H_2O		0.37
H_2		4.78
CO		2.83
CO_2		26.82
Cl		16.92
$\underline{n}$-C_2		3.90
$\underline{n}$-C_3		1.19
$\underline{n}$-C_4		0.52
$\underline{n}$-C_5		0.15
$\underline{n}$-C_6		0.03
$\underline{n}$-C_7		0.0081
$\underline{n}$-C_8		0.0017
$\underline{n}$-C_9		0.0005
$\underline{n}$-C_{10}		0.0002
$=C_2$		3.72
$=C_3$		4.50
$=C_4$		2.72
$=C_5$		1.05
$=C_6$		0.33
$=C_7$		0.115
$=C_8$		0.034
$=C_9$		0.0115
$=C_{10}$		0.0038
Pressure, psia	174	365 (inlet)
Temperature, °F	514	599 (inlet)
Space Velocity, $\frac{SCF_{FF}}{hr\text{-}ft^3 \text{ reactor}}$	280	959
Catalyst Concentration (lbs cat/ft^3 slurry)	4.44	-
$\frac{\text{lbs cat circulated}}{\text{sec.}}$	-	26,057

TABLE 8 (Continued)

Total Reactor ΔT, °F	-	36
CO Conversion, FF	91	97.8
Degree of Polymerization	4.0	3.3
Olefin-to-Paraffin Ratio	1.0	1.0
Gross CO_2 Molar Flow, moles/hr	73.4	5,133.6

TABLE 9

FREQUENCY FACTOR COMPARISON

Frequency Factor	Tube-Wall	Lathe Turning	Slurry	Fluid Bed
k_p^o [$(ft^3_{Rx})^2$/lb Cat-hr-mole]	73.0	113.0	2604.0	1821.0
k_H^o (ft^3_{Rx}/lb Cat-hr)	0.465	0.706	3.94	1.11
k_o^o(ft^3_{Rx}/lb Cat-hr)	0.0193	0.002	0.06	0.015
k_{WC}^o [$(ft^3_{Rx})^2$/lb Cat-hr-mole]	170.0	318.0	10,699.0	228.8

NORMALIZED FOR SURFACE AREA PER POUND OF CATALYST DIFFERENCES USING TUBE-WALL AS BASE

Frequency Factor	Tube-Wall	Lathe Turning	Slurry	Fluid Bed
k_p^o [$(ft^3_{Rx})^2$/lb Cat-hr-mole]	73.0	73.0	73.0	73.0
k_H^o (ft^3_{Rx}/lb Cat-hr)	0.465	0.070	0.110	0.045
k_o^o (ft^3_{Rx}/lb Cat-hr)	0.0193	0.00129	0.0016	0.0006
k_{WC}^o [$(ft^3_{Rx})^2$/lb Cat-hr-mole]	170.0	205.0	300.0	9.2

Note: All frequency factors are based on a reference temperature of 1100 °R.

TABLE 10

EXAMPLE EXPERIMENTAL RESULTS
FLAME SPRAYED CATALYST (FSC) FISCHER-TROPSCH RUNS

Item	Experiment No. HGR 33		Experiment No. HGR 34	
Catalyst Type	Coated Plates	Coated Plates	Coated Plates	Coated Plates
Fresh Gas Velocity, vol/vol/hr	600	1000	1000	2000
Fresh Feed Rate, scfh	165	275	275	550
Recycle Ratio Total Recycle ÷ Fresh Feed, vol/vol	51	15.9	20.4	14.4
Reactor Pressure, psig	400	400	400	400
Catalyst Temperature, °F				
Average	516	617	608	617
Differential	36	90	72	90
H_2 Conversion, %	73.4	90.9	90.1	83
CO Conversion, %	80.6	98.8	98.2	94.4
H_2 + CO Conversion, %	76.4	94.4	93.4	87.5
Overall Weight Balance, %	93.6	90.8	87.8	96.6
Hydrocarbons Recovered lb/1,000 scf fresh gas	7.4	9.5	10.3	11.6
Hydrocarbons Recovered, wt-%				
$C_1 + C_2$	59.7	36.5	33.9	29.5
C_3	6.6	14.1	13.3	12.8
Gasoline (C_3 = < 400 °F)	31.8	43.7	48.5	53.0
Diesel Fuel (400 to 600 °F)	1.9	5.0	4.0	3.8
Fuel Oil (600 to 842 °F)	0	0.4	0.2	0.5
Wax (> 842 °F)	0	0.3	0.1	0.4

TABLE 11

KEY REACTOR DESIGN BASIS ELEMENTS

Capacity, Btu/day Total Products HHV, billion	500
Pressure, psig	400
Temperature (average), °F	606
Space Velocity Factors	
J, scf/hr/sq ft of catalyst area	10
S_V, scf/hr/cu ft of reaction zone volume	1,330
Catalyst Activity	1.33
Syngas Composition	
Fresh Feed H_2:CO Ratio	1.45
CO + H_2 Conversion, %	80
Reactor Recycle Ratio	
Volume Recycle Gas : Volume (CO + H_2)	
in Fresh Syngas Feed	1.5
Heat of Reaction at Reactor Conditions	
Btu/scf of (CO + H_2) Converted	72.8

REACTOR PRODUCT COMPOSITION

	Weight Percent
C_1, C_2, $C_2^=$	19.3
C_3, $C_3^=$	4.5
C_4, $C_4^=$	11.9
C_5, $C_5^=$, C_6	13.6
C_7, C_8, C_9	19.2
C_{10}, C_{11} to 640 °F BP	18.8
640 to 940 °F BP	7.3
Alcohols and Ketones	4.9
Acids	0.5
Total	100.00

TABLE 12

CONCEPTUAL FISCHER-TROPSCH REACTOR DESIGN
COMPARED WITH PETC EXPERIMENTAL DATA

Item	Experiment HCR 34		SLTC Experiment 26C	TWR Experiment FT-TW-1	Conceptual Design Basis
"J", scfh/sf Catalyst Surface	8.85	17.7	1.5	30	10.0
H_2:CO Ratio in Feed	1.41	1.41	1.45	3	1.45
Recycle Ratio	20.4	14.4	27.0	-	1.5
(CO + H_2) Conversion, %	93.4	87.5	80.0	52.0	80.0
Total Reaction Heat Calculated, Btu/sf/hr	583.0	1092.0	84.0	1100.0	563.0

TABLE 13

TUBE-WALL REACTOR DESIGN COMPARISON

OPERATING CONDITIONS	Parsons	UOP Model Prediction	
Case	Study	1	2
Inlet Temperature, °F	571	571	606
Coolant Temperature, °F	606	606	640
Pressure, psia	415	415	415
J Factor (FF), $ft^3/hr\text{-}ft^2$	10.0	10.0	5.38
GHSV (FF), hr^{-1}	1330	1331	716.2
Recycle Ratio	1.5	1.5	1.5
H_2/CO Ratio			
Fresh Feed	1.45	1.45	1.45
Combined Feed	2.17	2.17	2.03
Catalyst	Flame sprayed magnetite	K promoted, flame sprayed taconite	
YIELD INFORMATION			
CO Conversion, mol-%			
Fresh Feed	88.7	34.9	90.0
Combined Feed	55.6	21.9	54.4
Degree of Polymerization	4.30	5.92	4.30
CO + H_2 Conversion, mol-%	53.3	18.8	41.1

TABLE 14

REACTOR COMPARISON

	Base				Per Mole $CO + H_2$ Used		
	Tube-Wall	Entrained Bed	Slurry		Tube-Wall	Entrained Bed	Slurry
$\frac{\text{Moles } H_2}{\text{Mole FF}}$	0.35	0.60	0.29	$\frac{\text{Moles } H_2}{\text{Mole } CO + H_2 \text{ Used}}$	0.55	0.69	0.37
$\frac{\text{Moles CO}}{\text{Moles FF}}$	0.29	0.27	0.49	$\frac{\text{Moles CO}}{\text{Mole } CO + H_2 \text{ Used}}$	0.45	0.31	0.63
$\frac{\text{Mole } H_2O}{\text{Mole FF}}$	0.12	0.27	0.0084	$\frac{\text{Moles } H_2O}{\text{Mole } CO + H_2 \text{ Used}}$	0.19	0.31	0.011
$\frac{\text{Moles } CO_2}{\text{Mole FF}}$	0.09	0.0	0.24	$\frac{\text{Moles } CO_2}{\text{Mole } CO + H_2 \text{ Used}}$	0.14	0.0	0.31
$\frac{\text{Lbs HC}}{\text{Mole FF}}$	2.90	3.92	3.56	$\frac{\text{Lbs HC}}{\text{Mole } CO + H_2 \text{ Used}}$	4.53	4.51	4.56

TABLE 15

YIELDS VERSUS REACTOR LENGTH

Tube-Wall Reactor		H_2/CO, FF = 2.0		
Once Through		Temperature, °F = 640		
CO Conversion = 98.3%		Pressure, psig = 415		
Relative Reactor Position	0	0.2	0.8	1.0
Yields				
H_2 (Mole Fraction)	0.645	0.522	0.406	0.374
CO (Mole Fraction)	0.323	0.133	0.012	0.010
Total Olefins	0	0.017	0.029	0.030
Degree of Polymerization	6.01	4.70	4.32	4.32

FIGURE 1

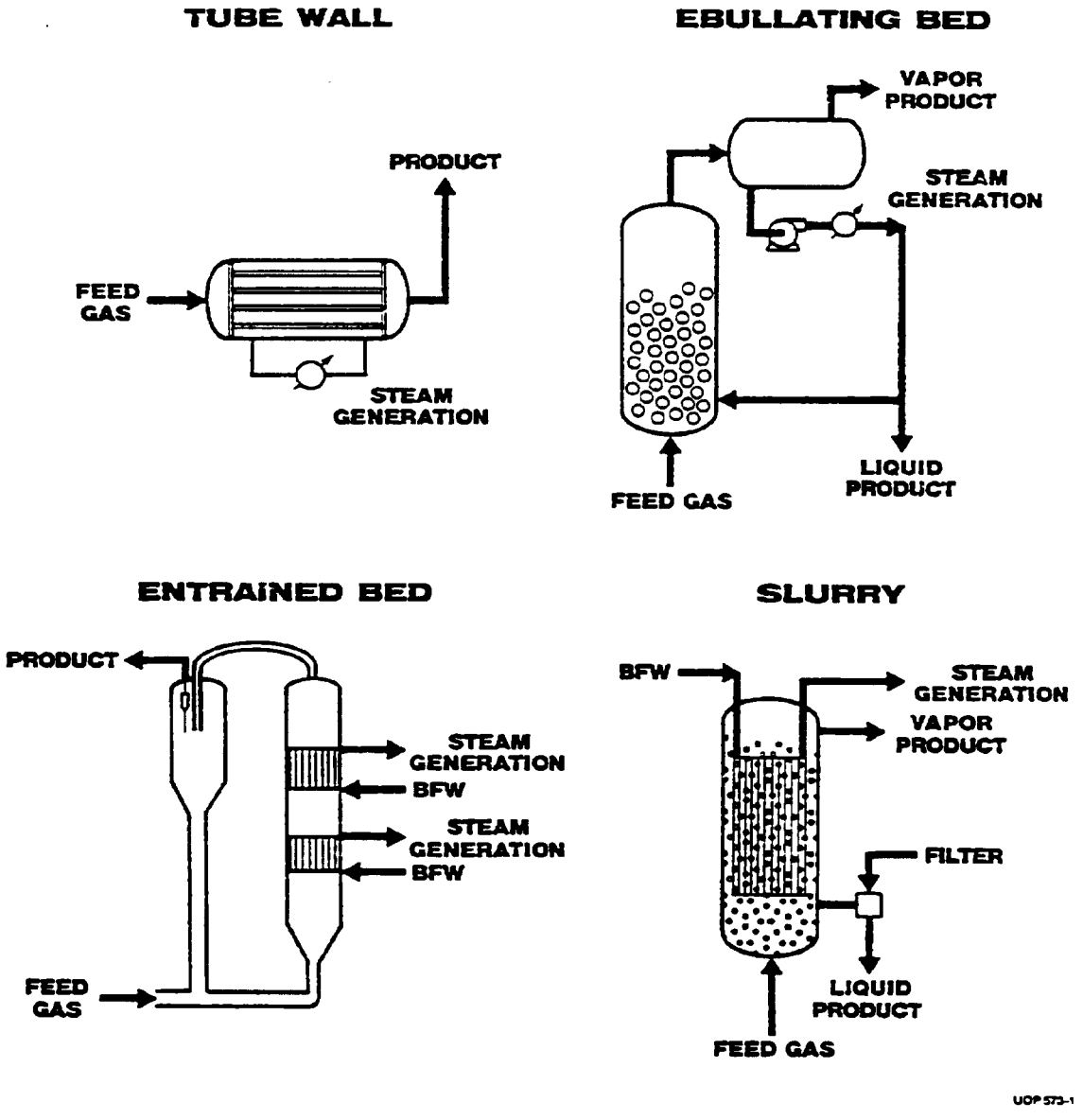
TUBE WALL
PRODUCT
FEED GAS
STEAM GENERATION
EBULLATING BED
VAPOR PRODUCT
STEAM GENERATION
LIQUID PRODUCT
FEED GAS
ENTRAINED BED
PRODUCT
STEAM GENERATION
BFW
STEAM GENERATION
BFW
FEED GAS
SLURRY
BFW
STEAM GENERATION
VAPOR PRODUCT
FILTER
LIQUID PRODUCT
FEED GAS
UOP 573-1

FIGURE 2

MECHANISM

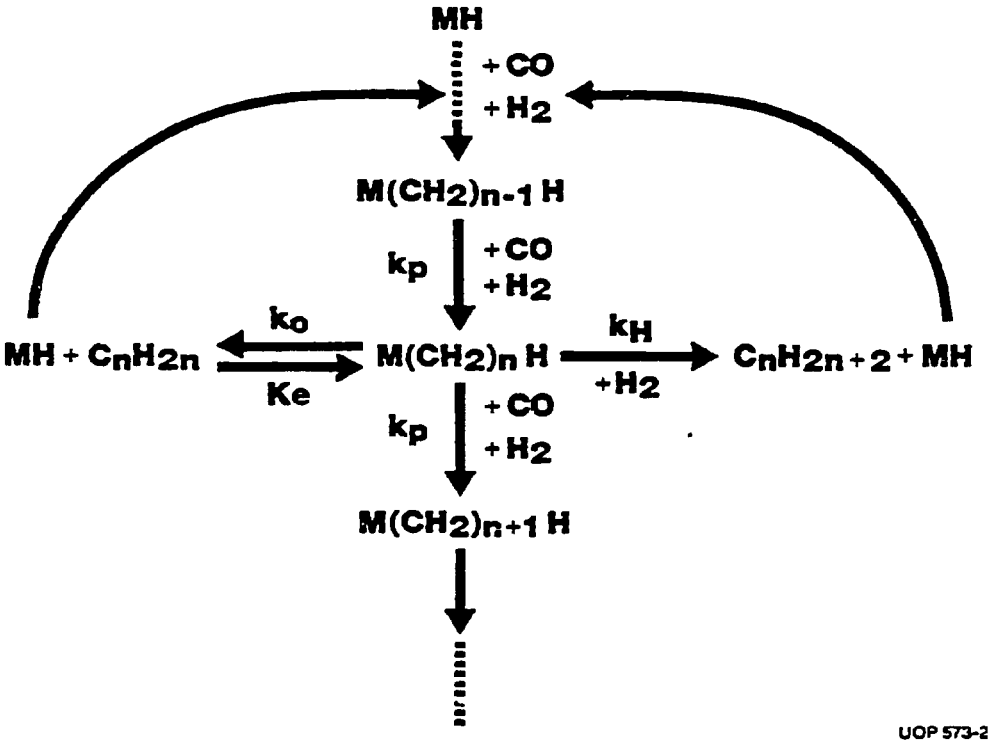

UOP 573-2

FIGURE 3

LOG OF MOLE FRACTION vs. CARBON NUMBER

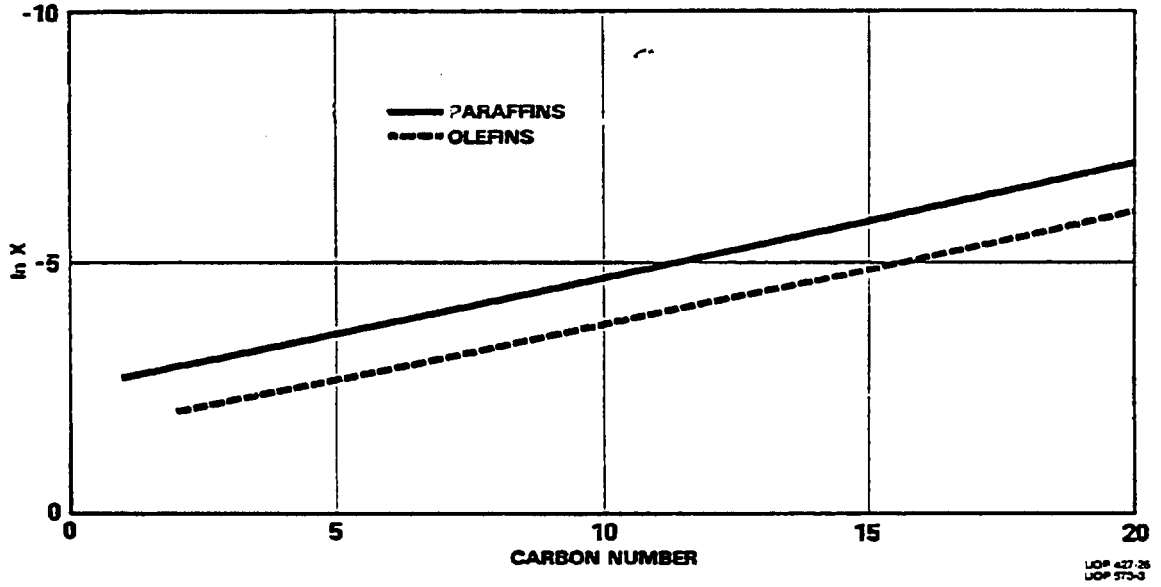

FIGURE 4

LOG OF MOLE FRACTION vs. CARBON NUMBER

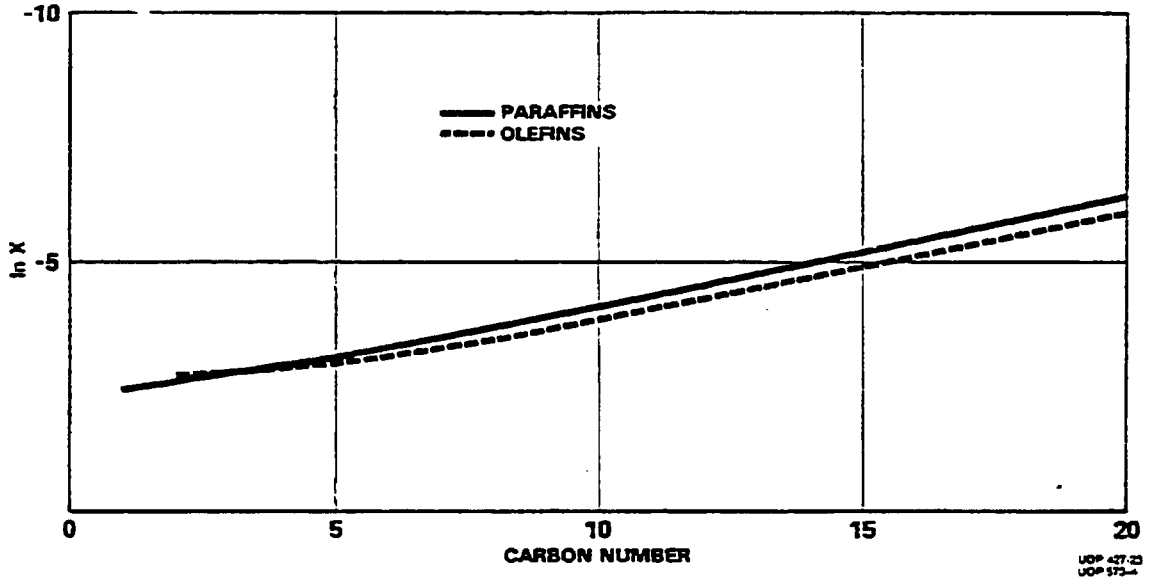

FIGURE 5

VARIATION OF TYPICAL PRODUCT SPLIT WITH DEGREE OF POLYMERIZATION

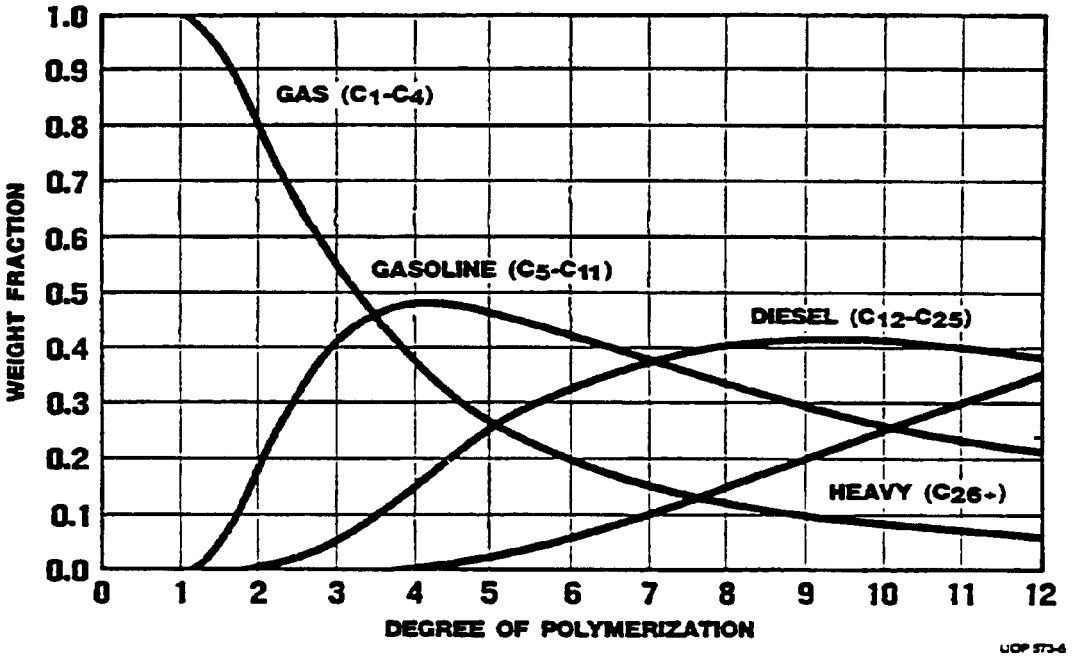

FIGURE 6

FISCHER-TROPSCH
ENTRAINED BED REACTOR
CO CONVERSION vs. REACTOR ΔT

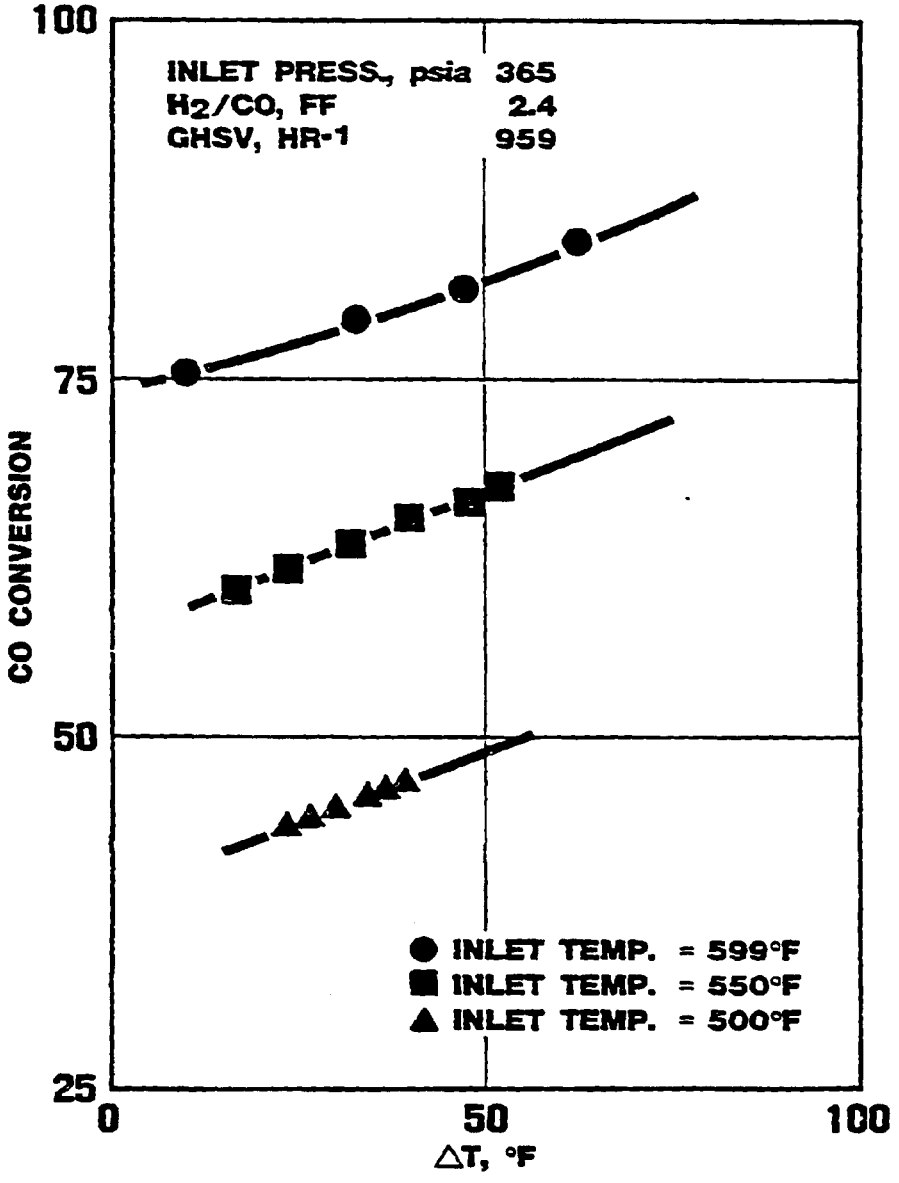

FIGURE 7

FISCHER-TROPSCH

ENTRAINED BED REACTOR
DEGREE OF POLYMERIZATION vs. REACTOR ΔT

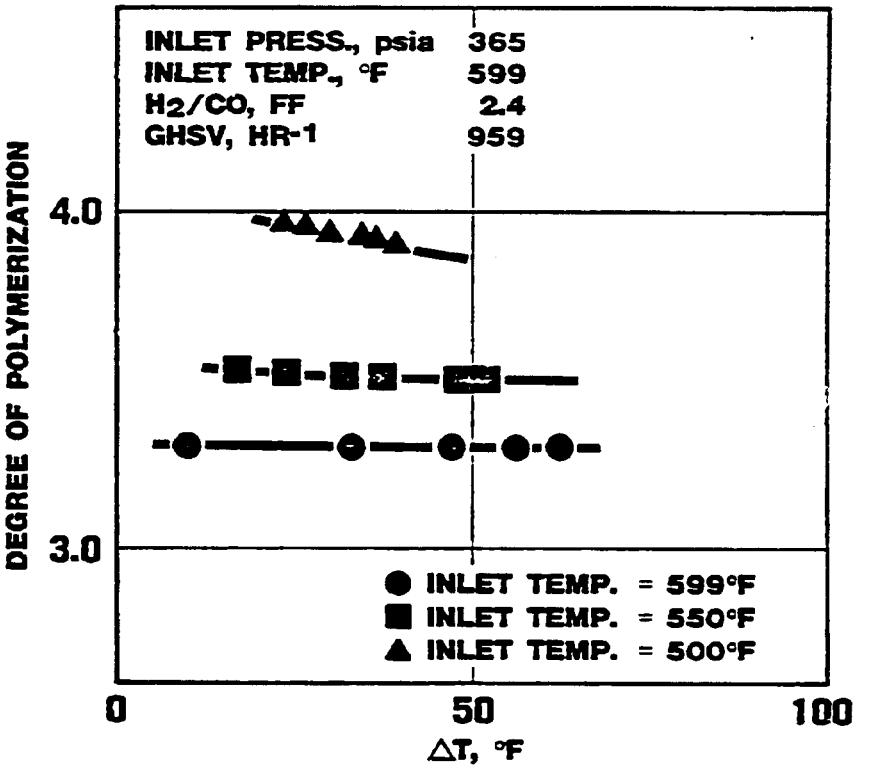

FIGURE 8

FISCHER-TROPSCH

ENTRAINED BED REACTOR AVERAGE CATALYST DENSITY vs. CATALYST CIRCULATION RATE

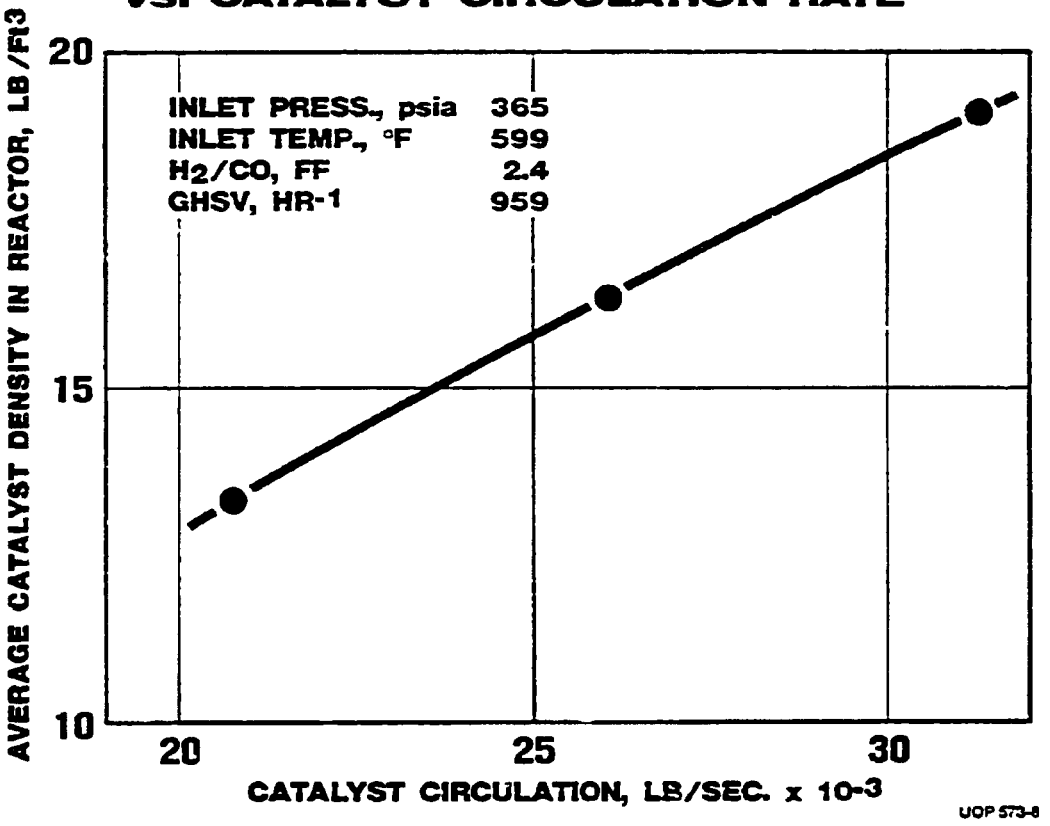

FIGURE 9

FISCHER-TROPSCH

ENTRAINED BED REACTOR
CO CONVERSION vs. CATALYST CIRCULATION
DEGREE OF POLYMERIZATION vs. CATALYST CIRCULATION

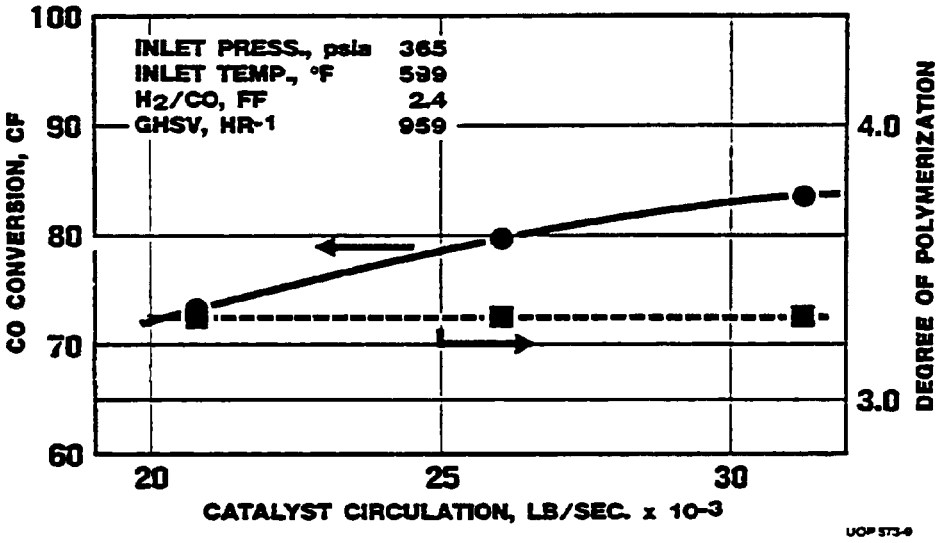

FIGURE 10

FISCHER-TROPSCH

ENTRAINED BED REACTOR
CO CONVERSION vs. β
DEGREE OF POLYMERIZATION vs. β

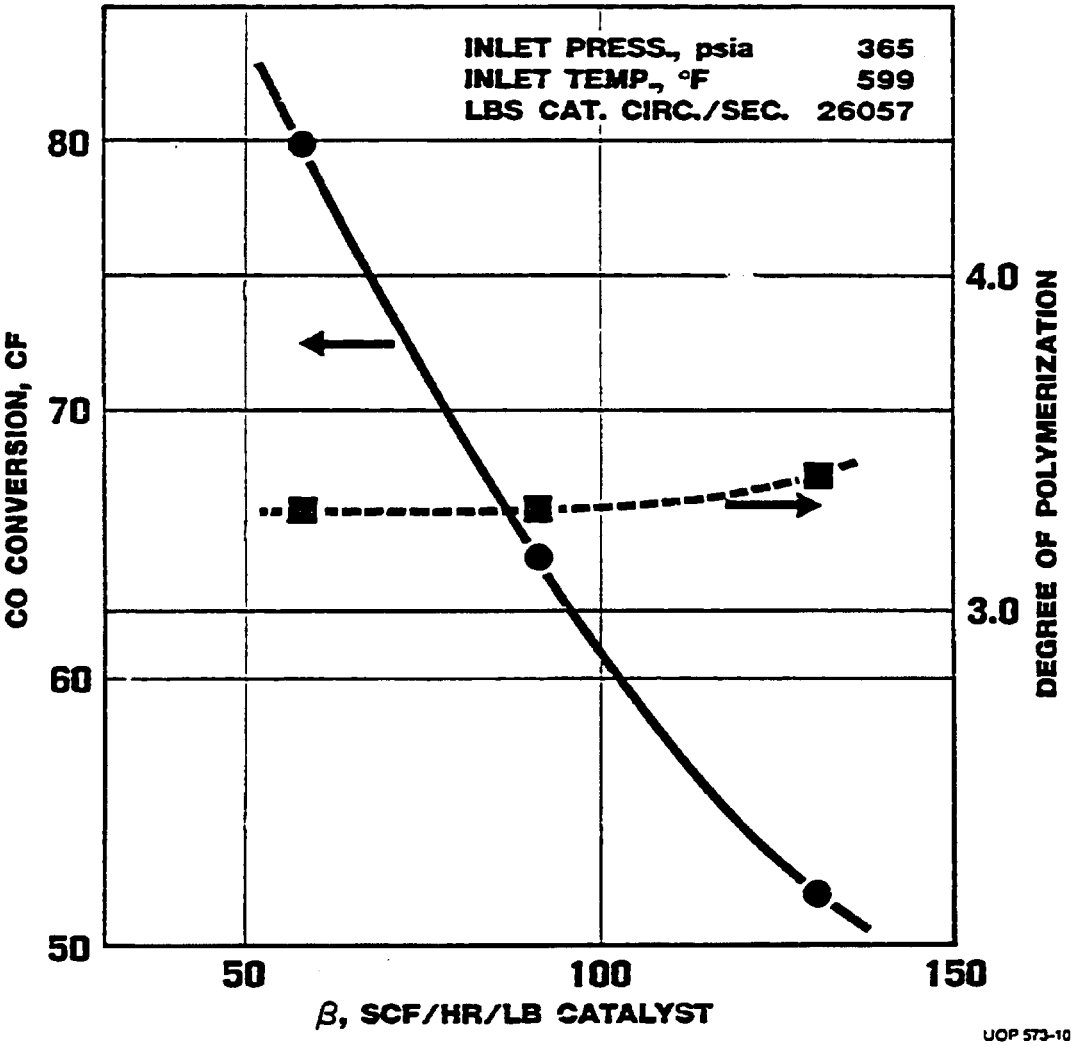

FIGURE 11

FISCHER-TROPSCH

SLURRY REACTOR
CO CONVERSION vs. TEMPERATURE

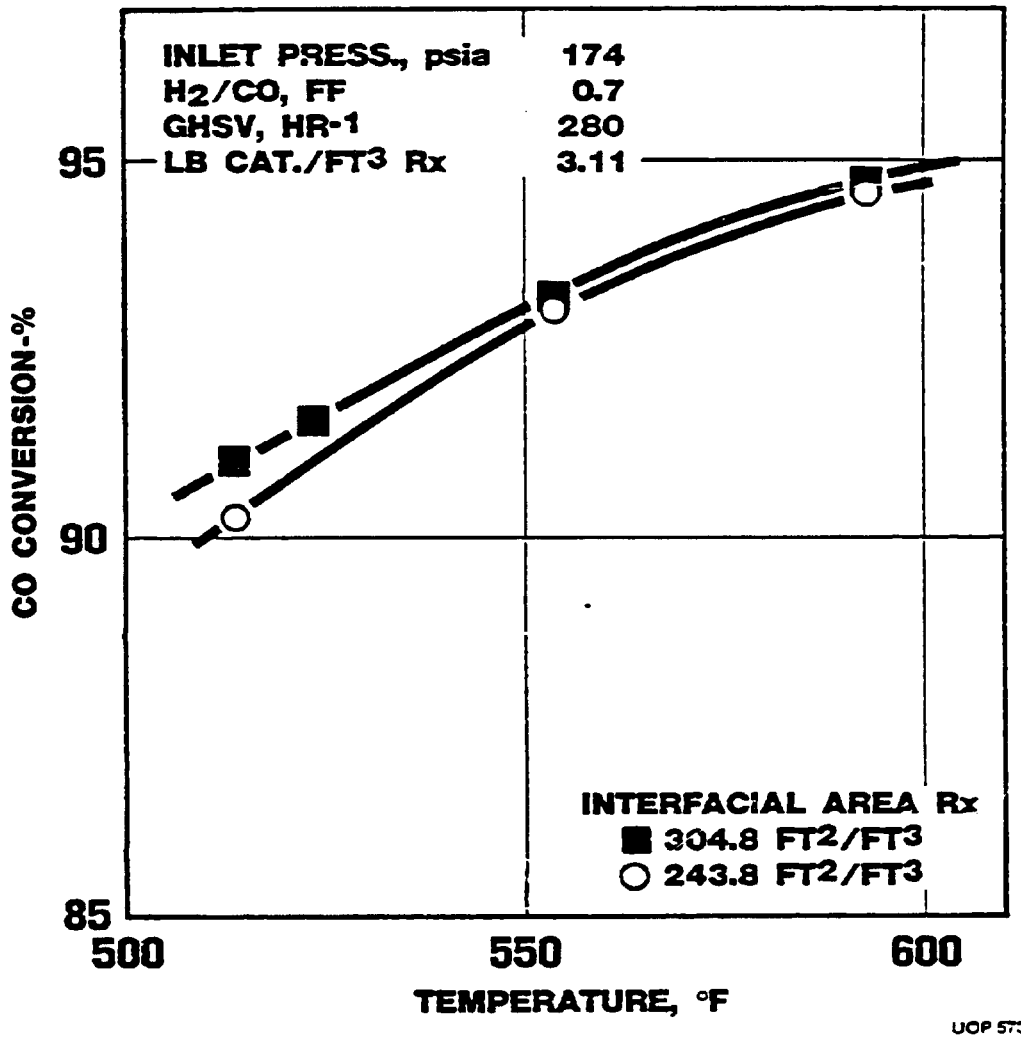

UOP 573-11

FIGURE 12

FISCHER-TROPSCH

SLURRY REACTOR
DEGREE OF POLYMERIZATION
vs. TEMPERATURE

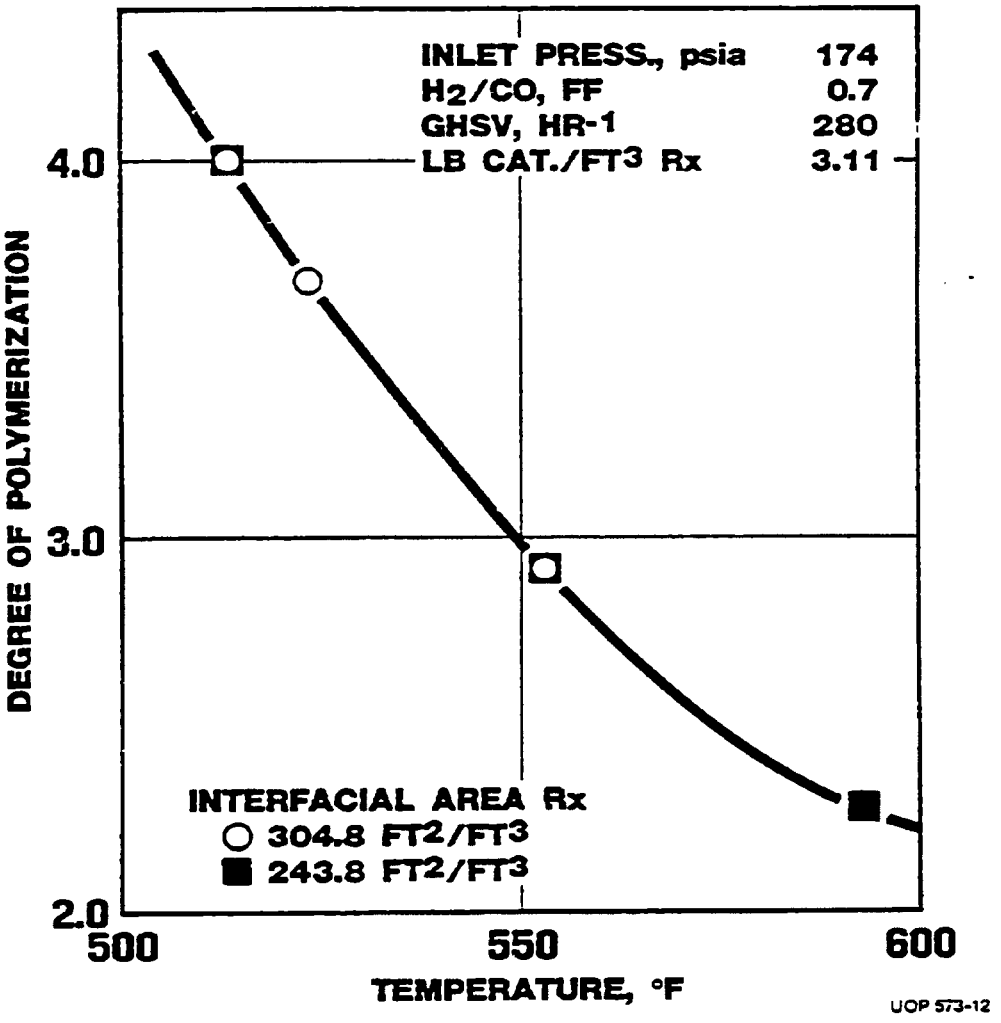

UOP 573-12

FIGURE 13

FISCHER-TROPSCH

SLURRY REACTOR SYSTEM
CO CONVERSION AND DEGREE OF POLYMERIZATION vs. RELATIVE MASS TRANSFER RATE CONSTANTS

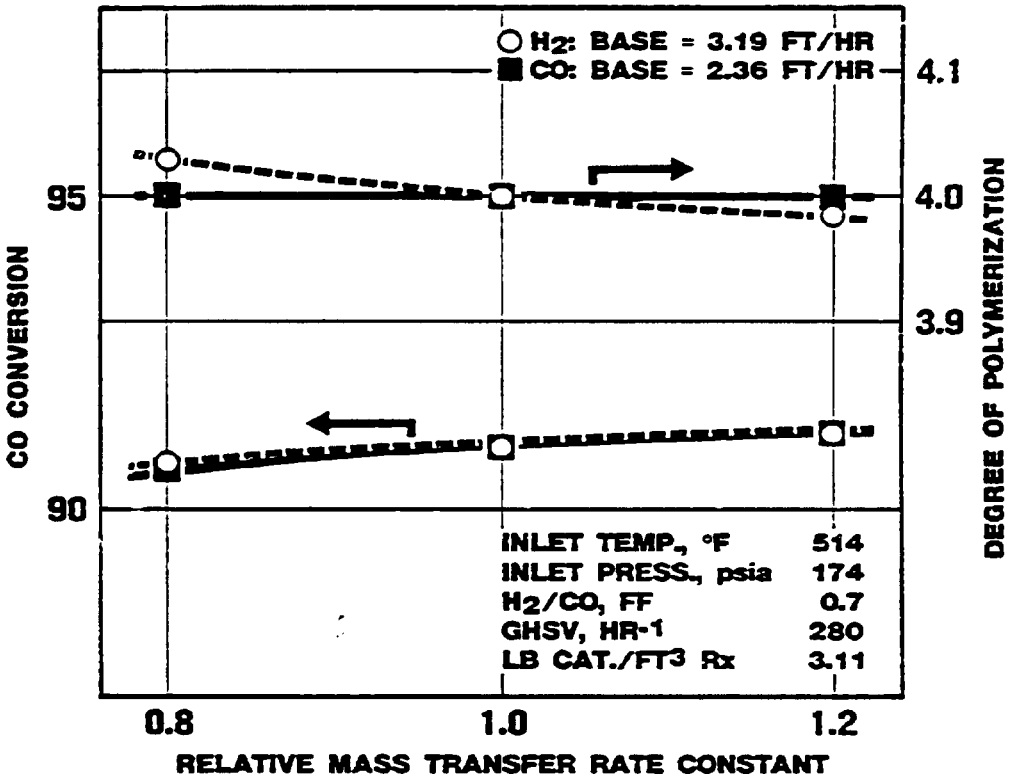

FIGURE 14

FISCHER-TROPSCH

REACTOR COMPARISON
DEGREE OF POLYMERIZATION vs. TEMPERATURE